Pineal-specific agouti protein regulates teleost background adaptation

Chao Zhang[a], Youngsup Song[b], Darren A. Thompson[c], Michael A. Madonna[c], Glenn L. Millhauser[c], Sabrina Toro[d], Zoltan Varga[d], Monte Westerfield[d], Joshua Gamse[e], Wenbiao Chen[a], and Roger D. Cone[a,1]

[a]Department of Molecular Physiology and Biophysics, The Vanderbilt University School of Medicine, Nashville, TN 37232; [b]The Salk Institute for Biological Sciences, La Jolla, CA 92037; [c]Department of Chemistry and Biochemistry, University of California, Santa Cruz, CA 95064; [d]Institute of Neuroscience, University of Oregon, Eugene, OR 97403; and [e]Department of Biological Sciences, The Vanderbilt University Medical Center, Nashville, TN 37232

This contribution is part of the special series of Inaugural Articles by members of the National Academy of Sciences elected in 2010.

Contributed by Roger D. Cone, October 6, 2010 (sent for review August 30, 2010)

Background adaptation is used by teleosts as one of a variety of camouflage mechanisms for avoidance of predation. Background adaptation is known to involve light sensing by the retina and subsequent regulation of melanophore dispersion or contraction in melanocytes, mediated by α-melanocyte–stimulating hormone and melanin-concentrating hormone, respectively. Here, we demonstrate that an agouti gene unique to teleosts, *agrp2*, is specifically expressed in the pineal and is required for up-regulation of hypothalamic *pmch* and *pmchl* mRNA and melanosome contraction in dermal melanocytes in response to a white background. *floating head*, a mutant with defective pineal development, exhibits defective up-regulation of *mch* mRNAs by white background, whereas *nrc*, a blind mutant, exhibits a normal response. These studies identify a role for the pineal in background adaptation in teleosts, a unique physiological function for the agouti family of proteins, and define a neuroendocrine axis by which environmental background regulates pigmentation.

pigmentation | camouflage | zebrafish

Camouflage mechanisms are widely used across all orders of the animal kingdom. Although mammals have evolved coat patterning to aid in escaping predation or stalking prey, regulated camouflage, such as the seasonal pelage change in the arctic hare, occurs slowly because shedding and growth of a new coat is required. In contrast, reptiles, amphibians, and teleosts can more rapidly alter skin color to match their surroundings.

One neural circuit involved in nonvisual phototransduction is the retinohypothalamic tract. A class of intrinsically photosensitive retinal ganglion cells (ipRGCs) project to anterior hypothalamic nuclei, such as the suprachiasmatic nucleus (SCN) (1). This non–image-forming photoreceptive pathway is independent of rod and cone photoreceptors and is sufficient to provide the photic input necessary to entrain the circadian clock to the environmental light–dark cycle (2). Blind transgenic mice lacking rods and cones retain normal photic entrainment of circadian rhythms, for example (2, 3). Melanopsin seems to be the primary photopigment in mammalian ipRGCs involved in nonvisual photoreception regulating circadian entrainment, the sleep–wake cycle, and the pupillary light reflex (4, 5).

In mammals, both visual and nonvisual photoreception requires the retina, and the pineal gland receives photic input indirectly, via projections from the SCN that receive direct retinal inputs. In contrast, in nonmammalian vertebrates photoreceptors are found in both the pineal and the skin; melanopsin was originally identified, for example, in dermal melanocytes of *Xenopus laevis* (6). A variety of opsin molecules are found in the pineal organ of nonmammalian vertebrates, including exo-rhodopsin, pinopsin, parapinopsin, and vertebrate ancient opsin (5). In many species of teleosts background adaptation is regulated in part by the pineal gland: shining light specifically on the pineal causes skin lightening, whereas covering the area of the pineal with India ink causes skin darkening (7).

An important mechanism in the pigmentary response to photic information involves the dispersion or aggregation of pigment granules, or melanophores, in dermal melanocytes via the actions of the pituitary peptide α-MSH (melanocyte-stimulating hormone) and hypothalamic peptide MCH (melanocyte-concentrating hormone), respectively (8, 9). The secretory activity of α-MSH–expressing cells of the pituitary increases in response to a black background (10), and serum α-MSH levels increase as well (11). MCH in teleosts is found in secretory neurophysiotrophic neurons in the lateral tuberal nuclei (NLT) of the hypothalamus, an arcuate nucleus equivalent. In contrast to regulation of α-MSH, exposure to a white background elevates MCH in the NLT in a variety of fish species (12), including the zebrafish (13), and can produce a measurable increase in serum MCH. Thus, background adaptation involves a classic neuroendocrine pathway.

In nonmammalian vertebrates, the pineal gland is not only an endocrine gland releasing melatonin but also a photosensory organ, with secondary afferent neurons that innervate a variety of brain regions, comparable to the retinal ganglion cells (14). Indeed, in the zebrafish, pineal and retinal neurons send projections to a number of nuclei in common, including sites in the anterior hypothalamus, such as the SCN (15). SCN neurons, in turn, are hypophysiotrophic in teleosts, and thus the pineal, through its projections to the SCN, provides a second neuroanatomical pathway through which light can regulate pigmentation.

The agouti proteins are small secreted molecules (16–19) that act as endogenous antagonists of the melanocortin receptors (18, 20, 21), a family of G protein–coupled receptors. Two agouti genes are found in mammals, agouti (ASP) (16, 17), which regulates the eumelanin–pheomelanin switch in mammalian pelage, and agouti-related protein (AgRP), which is expressed in the CNS and regulates energy homeostasis (18, 19). A third agouti gene, *agrp2*, has been identified now in several fish species, including zebrafish, trout, tetraodon, and torafugu (22). We show here that teleost *agrp2* is expressed specifically in the pineal gland, regulates the hypothalamic proMCH and proMCH-like genes (*pmch* and *pmchl*), and is required for melanosome aggregation in response to environmental background, thus elucidating a pineal–hypothalamic neuroendocrine pathway by which light regulates pigmentation.

Results

***agrp2* Is Expressed in the Pineal Gland and Is Not Regulated by Metabolic State.** To determine the physiological functions of the teleost-specific agouti protein AgRP2, we first examined the

Author contributions: C.Z., Y.S., G.L.M., M.W., J.G., W.C., and R.D.C. designed research; C.Z., Y.S., D.A.T., M.A.M., S.T., and Z.V. performed research; G.L.M., M.W., and J.G. contributed new reagents/analytic tools; G.L.M., M.W., J.G., W.C., and R.D.C. analyzed data; and R.D.C. wrote the paper.

The authors declare no conflict of interest.

Freely available online through the PNAS open access option.

[1]To whom correspondence should be addressed. E-mail: roger.cone@vanderbilt.edu.

This article contains supporting information online at www.pnas.org/lookup/suppl/doi:10.1073/pnas.1014941107/-/DCSupplemental.

distribution of *agrp2* mRNA in zebrafish embryos [72–96 h postfertilization (hpf)], viewed laterally (Fig. 1*A*) or dorsally (Fig. 1*B*) by in situ hybridization to whole mounts, or viewed dorsally in thin sections (Fig. 1*C*); *agrp2* mRNA is detected exclusively in the pineal gland. Real-time quantitative PCR (qPCR) analysis with adult zebrafish tissues confirmed that *agrp2* mRNA is also expressed most strongly in brain, with lower levels seen in skin, muscle, and testis (Fig. 1*D*).

Both mammalian and teleost *agrp* are regulated by metabolic state (23), thus we examined whether *agrp2* was under similar regulatory control. Compared with the control-fed group, a 15-d fast significantly up-regulated *agrp* mRNA expression by eightfold in the brain of male fish (Fig. 1*E*), comparable to results previously published for the female fish (23). In contrast, no significant change in *agrp2* mRNA levels was observed (Fig. 1*F*). Consistent with the pineal-specific expression of *agrp2*, we identified pineal-specific enhancer elements, such as the photoreceptor-conserved element (PCE), E-box, and pineal expression-promoting element (PIPE), upstream of the *agrp2* coding sequence (Fig. S1*A*). The developmental expression of *agrp2* by both whole-mount in situ hybridization and qPCR was also examined. Both procedures detected *agrp2* mRNA by 2 d postfertilization (dpf) (Fig. S1 *B*–*F*).

AgRP2 Is a Competitive Antagonist of the Zebrafish MC1-R. In mammals, AgRP is a selective antagonist of the melanocortin receptors MC3R and MC4R, expressed primarily in the CNS (18, 21). Using HEK293 cells expressing recombinant zebrafish melanocortin receptors, we showed previously that mouse $AgRP_{(82–131)}$ can competitively decrease α-MSH–mediated cAMP production, with high efficacy at MC1R, MC3R, and MC4R (24). Here, we tested the pharmacological potency of synthetic zebrafish AgRP and AgRP2 at the zebrafish melanocortin receptors. HEK-293 cells stably expressing zebrafish melanocortin receptors were incubated with serial dilutions of α-MSH in the presence or absence of the folded, cysteine-rich C-terminal domain of $AgRP_{(83–127)}$ or $AgRP2_{(93–136)}$, which are comparable to the biologically active human $AgRP_{(87–132)}$ (25). $AgRP_{(83–127)}$ blocked MC1R, MC3R, and MC4R, and less potently, MC5Ra and MC5Rb (Fig. 2 *A*, *C*, *E*, *G*, and *I*). On the other hand, $AgRP2_{(93–136)}$ was a potent antagonist of the MC1R but showed little activity at MC4R (Fig. 2 *B* and *F*) and no antagonist activity at MC3R (Fig. 2*D*). Together with the data on regulation of *agrp2* gene expression, these findings imply distinct roles for AgRP and AgRP2.

***Agrp2* Expression Is Required for Up-Regulation of *mch* and *mchl* and Melanosome Contraction Induced by a White Background.** To examine the functional consequences of *agrp2* expression directly, we first characterized the background adaptation response of

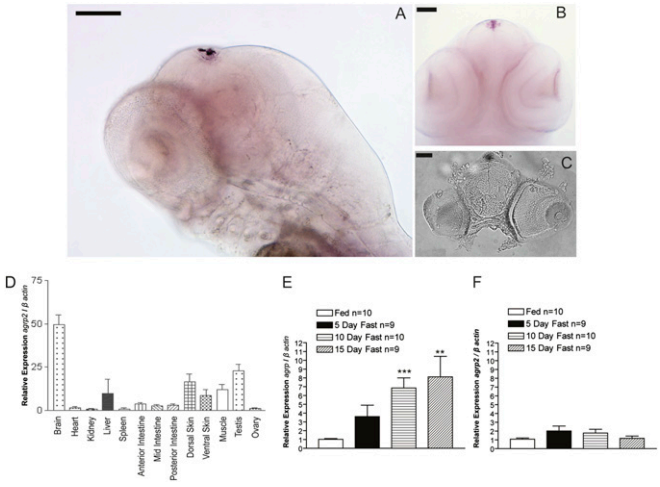

Fig. 1. *agrp2* is expressed in the zebrafish pineal gland and is not regulated by metabolic state. (*A*) Lateral view of a 96-hpf whole-mount embryo. Whole-mount in situ hybridization was performed with dig-*agrp2* antisense probe followed by Nitro blue tetrazolium chloride/ 5-Bromo-4-chloro-3-indolyl phosphate (NBT/BCIP) color development. (*B*) Dorsal view of a 72-hpf embryo. (*C*) Frontal view of a 20-μm section from a 96-hpf embryo hybridized as described in *A*, then embedded in optimal cutting temperature compound and processed using a cryostat. (*D*) qPCR analysis of *agrp2* with tissues from four adult zebrafish (two male and two female). *agrp2* mRNA expression was normalized to *β-actin* mRNA. (*E* and *F*) Relative expression levels of *agrp* and *agrp2* by metabolic state as analyzed by qPCR. One-year-old male fish were fed or fasted for indicated times, and the relative mRNA expression levels of *agrp* and *agrp2* normalized to *β-actin* were determined from whole-brain tissues. Results are expressed as mean ± SEM, and statistical analyses were done by unpaired *t* test. $^{**}P < 0.01$; $^{***}P < 0.001$. (Scale bars in *A*–*C*: 100 μm.)

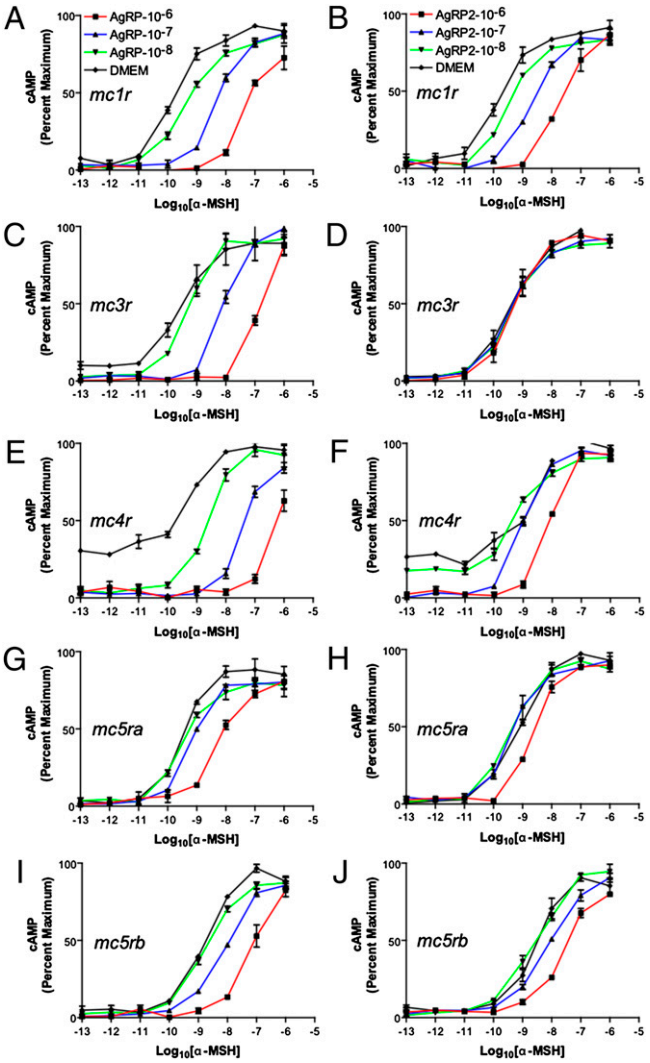

Fig. 2. Pharmacological activity of zebrafish $AgRP_{(83–127)}$ and $AgRP2_{(93–136)}$ peptides. The left column of graphs (*A*, *C*, *E*, *G*, and *I*) shows dose–response curves for α-MSH in the presence of 10^{-6} M (squares, red lines), 10^{-7} M (triangles, blue lines), 10^{-8} M (inverted triangles, green lines), or absence (diamonds, black lines) of $AgRP_{(83–127)}$ peptide at the zebrafish melanocortin receptors indicated. The right column of graphs (*B*, *D*, *F*, *H*, and *J*) shows dose–response curves for α-MSH in the presence of the same doses of $AgRP2_{(93–136)}$ peptide. α-MSH–stimulated activity of zebrafish melanocortin receptors was monitored using a cAMP-dependant β-galactosidase assay. Data points indicate the averages of triplicate determinations. Experiments were performed in triplicate, and graphs were drawn and analyzed using Graphpad Prism.

zebrafish embryos cultured on white, gray, or black backgrounds from fertilization until 4 dpf. As seen in Fig. 3 *A–C*, individual melanocytes increased in apparent size and pigmentation in response to the increased darkness of the background. The identity of the pigmented spots as individual melanocytes was validated by identification of individual nuclei under high magnification using a compound microscope (Fig. S2). Furthermore, as shown previously for adult zebrafish (13), both zebrafish MCH genes, *pmch* and *pmchl*, were expressed at higher levels when the embryos were grown on lighter backgrounds (Fig. 3 *D–I*), as examined by whole-mount in situ hybridization. qPCR, performed on whole embryos, confirmed this finding, demonstrating a 2.9- and 5.2-fold increase in *pmch* and *pmchl*, respectively, in fish on a white vs. black background (Fig. 3*J*). In contrast to *pmch* and *pmchl*, the agouti genes *asp*, *agrp*, and *agrp2* did not seem to be potently up-regulated in embryos exposed to a white background (Fig. S3). These data validated the use of embryos for study of background adaptation and allowed us to then use morpholino knockdown technology to assess the role of various genes in this physiological response.

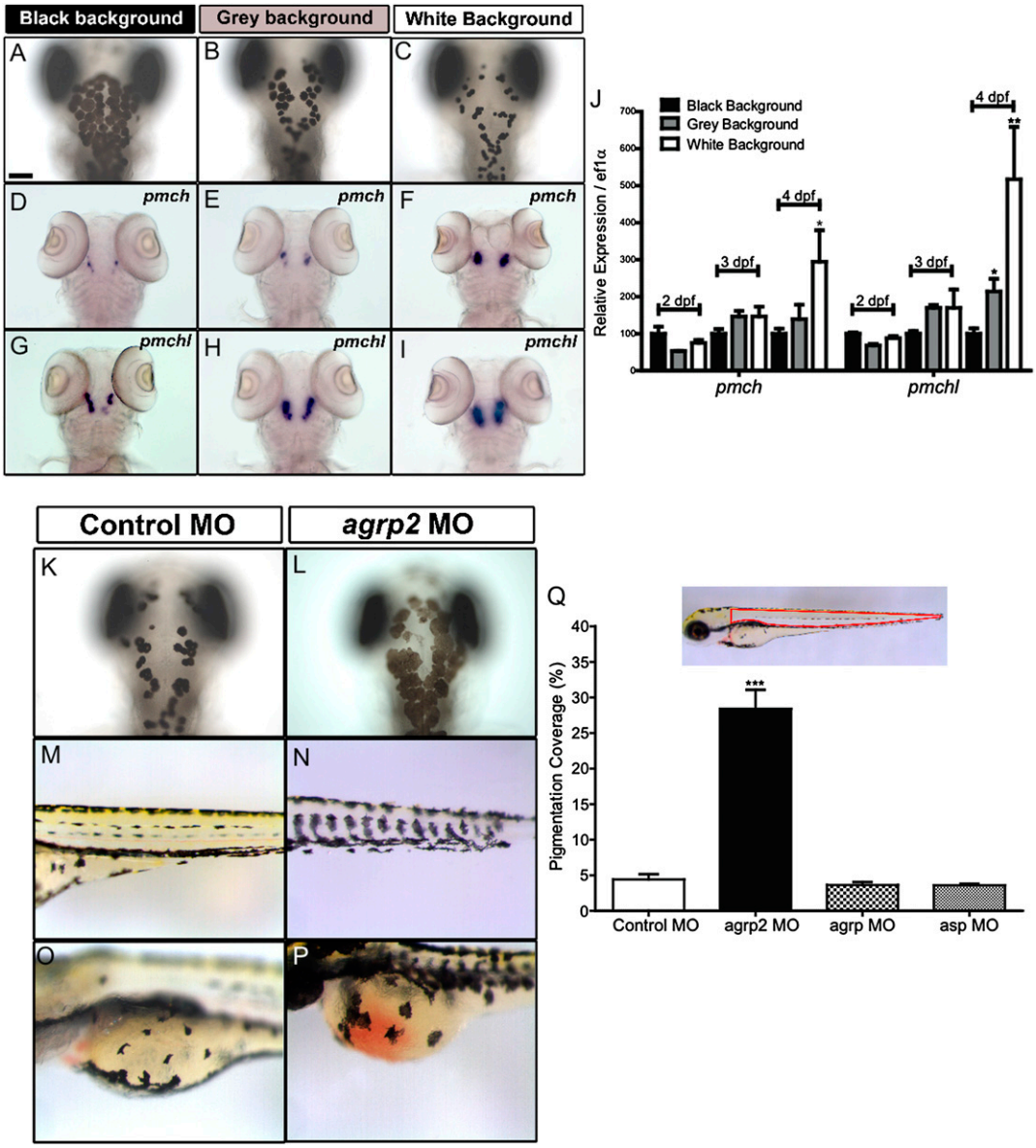

Fig. 3. *agrp2* is required for melanosome contraction in zebrafish. Control or morpholino-injected embryos were kept in black-, gray-, or white-bottomed Petri dishes with 14-h/10-h light/dark cycle at 28 °C upon fertilization. (*A–C*) Dorsal melanocytes of (*A*) black, (*B*) gray, or (*C*) white background-adapted wild-type embryos at 4 dpf. (*D–I*) Whole-mount in situ hybridization of (*D–F*) *pmch* and (*G–I*) *pmchl* in black (*D* and *G*), gray (*E* and *H*), or white (*F* and *I*) background-adapted wild-type embryos at 4 dpf. At least 30 embryos for each condition were analyzed. Scale bar: 100 μM. (*J*) Relative expression levels of *pmch* and *pmchl* were analyzed by real-time qPCR. At 2, 3, and 4 dpf, 30 black, gray, or white background-adapted wild-type embryos were divided into three groups and killed for RNA extraction and cDNA synthesis. mRNA expression was normalized to *ef1α* mRNA. Results are expressed as mean ± SEM, and statistical analysis was done by unpaired *t* test. $*P < 0.05$; $**P < 0.01$. (*K–P*) MOs designed to inhibit expression of each of the zebrafish agouti proteins were injected into wild-type zebrafish embryos. Dermal melanocytes were examined at 3–5 dpf at 1200 hours. Photographs show the (*K* and *L*) dorsal head, (*M* and *N*) lateral trunk, and (*O* and *P*) yolk melanocytes in inverted control (*K*, *M*, and *O*) or *agrp2* (*L*, *N*, and *P*) antisense MO-injected embryos at 4 dpf at 1200 hours. (*Q*) Melanosome coverage of the lateral trunk was quantified at 4 dpf using ImageJ (National Institutes of Health) on *agrp2* ATG MO-injected (28.4%, $n = 10$), *agrp* ATG MO-injected (3.6%, $n = 10$), and *asp* ATG MO-injected (3.5%, $n = 10$) embryos compared with inverted control MO-injected embryos (4.4%, $n = 10$). Error bar indicates ± SEM. Statistical significance tested by unpaired *t* test. $***P < 0.001$.

We next injected zebrafish zygotes with morpholino oligonucleotides (MO) directed against the different zebrafish agouti mRNAs and examined fish at 3–5 dpf. Injection of control morpholinos (Fig. 3 *K*, *M*, and *O*) had no impact on pigmentation. In contrast, injection of morpholinos against *agrp2* induced dispersion of melanosomes in dermal melanocytes (Fig. 3 *L*, *N*, and *P*). Injection with a morpholino against *agrp2* increased the area of lateral trunk that was melanized from 4.4% to 28.4%, whereas morpholinos against *agrp* or *asp* had no effect relative to control (Fig. 3*Q*). Maintenance of adult zebrafish on a white background has been shown to up-regulate *pmch* and *pmchl* mRNA levels and induce melanosome aggregation (13), and we have demonstrated the same phenomenon in embryos (Fig. 3*J*). The dispersion of melanosomes by *agrp2* morpholino injection into zebrafish zygotes (Fig. 3) suggested that *agrp2* expression might be required for up-regulation of *pmch* and *pmchl* mRNA levels in response to a white background. We examined the effect of *agrp2* on expression of *pmch* and *pmchl* in two different ways. First, qPCR was used to examine *pmch* (Fig. 4*A*) and *pmchl* (Fig. 4*B*) expression after injection of MO into zebrafish zygotes maintained on a white background. Two different morpholinos against *agrp2*, designed against either the 5′ UTR or the start of translation, potently reduced *pmch* and *pmchl* mRNA levels of fish raised on a white background, whereas control, *asp*, or *pomca* morpholinos had no apparent effect. In an independent experiment, the number of detectable *pmch* and *pmchl* neurons in the hypothalamus was examined by whole-mount in situ hybridization with *pmch*- and *pmchl*-specific probes after injection of the MO indicated (Fig. 4*C*). Individual neurons were counted at high magnification in 14–22 animals from each treatment group. The quantitation of detectable number of neurons yielded data similar to quantitation by qPCR, with *agrp2* morpholinos most potently decreasing the number of detectable *pmch* (Fig. 4*D*) and *pmchl* (Fig. 4*E*) neurons. Some decrease in detectable *pmch* and *pmchl* neurons was observed with *agrp* morpholinos as well. Importantly, knockdown of *agrp2* does not nonspecifically reduce gene expression in the zebrafish NLT, because no change in *pomca* gene, also expressed in the NLT, was seen after administration of *agrp2* morpholinos (Fig. S4). The dependency of melanosome contraction on MCH gene expression in embryos was also validated; dual morpholino knockdown of *pmch* and *pmchl* prevented contraction of melanosomes in embryos grown on a white background (Fig. S5).

Loss of Pineal in *floating head* Mutant Is Associated with a Defect in Melanosome Contraction and Up-regulation of *pmch and pmchl* After Exposure to a White Background. The *floating head* mutant (*flh*) is a strain of zebrafish in which pineal gland neurogenesis is blocked owing to the absence of a homeodomain-containing transcription factor encoded by the gene (26). Progeny of $flh^{+/-}$ heterozygous fish were raised in white-bottomed Petri dishes to 4 dpf. Homozygous $flh^{-/-}$ offspring were identified by their distinctive morphological defects (27). In comparison with phenotypically wild-type fish ($flh^{+/+}$ and $flh^{+/-}$), melanocytes were visibly expanded in $flh^{-/-}$ fish (Fig. 5 *A* and *B*). Detectable levels of *agrp2* were not observed in $flh^{-/-}$ fish (Fig. 5 *C* and *D*). In contrast, no changes in hypothalamic *agrp* or *pomca* were detected in $flh^{-/-}$ fish in comparison with WT animals (Fig. 5 *E*, *F*, *K*, and *L*). In parallel with the absence of *agrp2* mRNA, hypothalamic *pmch* and *pmchl* levels in $flh^{-/-}$ fish were visibly reduced relative to wild-type ($flh^{+/+}$ and $flh^{+/-}$) animals (Fig. 5 *G*–*J*). qPCR data confirmed the findings observed by whole-mount in situ hybridization (Fig. 5*M*).

Normal Melanosome Contraction and Up-Regulation of *pmch and pmchl* Observed in the Blind *no optokinetic response c* Mutant. Many blind zebrafish mutants have been isolated from N-ethyl-N-nitrosourea chemical mutagenesis by screening for defective responses in optomotor or optokinetic assays (28, 29). Many, but not all, blind mutants also exhibit defective background adaptation (29). Because pineal photoreceptors resemble retinal photoreceptors both structurally and functionally, it is possible that some gene products may be required both for retinal and pineal phototransduction. For example, photoreceptors seem to degenerate in both the retina and pineal of the *niezerka* mutant (30). In the blind mutant *no optokinetic response c* (*nrc*), however, pineal photoreceptors are reported to appear normal by electron microscopy (30). To test whether visual phototransduction plays a role in background adaption, we chose to study the process in this mutant. Offspring of $nrc^{+/-}$ matings were raised in black- or white-bottomed Petri dishes, and homozygous $nrc^{-/-}$ animals were picked on the basis of their imbalanced swimming behavior, another documented phenotype in the mutant. Just like sibling wild-type fish, $nrc^{-/-}$ mutants exhibited robust background adaptation (Fig. S6 *A*–*D*), with dispersed melanosomes on a black background (Fig. S6*C*) and contracted melanosomes (Fig. S6*D*) on a white background. Whole-mount in situ hybridization and qPCR data demonstrated that *agrp2* mRNA expression is similar in WT and $nrc^{+/-}$ and $nrc^{-/-}$ mutants and is not up-regulated by exposure to a white background (Fig. S6 *E*–*H* and *Q*). *pmch* and *pmchl* mRNA were significantly up-regulated as well in both wild-type and $nrc^{-/-}$ fish in response to white background (Fig. S6 *I*–*P* and *Q*).

Melanocortin-1 Receptor Is Expressed at Highest Levels in Zebrafish Hypothalamus. In mammals, the MC1R is expressed primarily in skin (31), where it acts directly to regulate the eumelanin–pheomelanin switch (32). In contrast, MC1R expression has been reported in the brain of several fish species (33, 34). AgRP2 is most potently an MC1R antagonist, with little activity at the MC4R and no activity at the MC3R (Fig. 2), yet it regulates *pmch* and *pmchl* expression in the hypothalamus. Furthermore, pineal neurons have been reported to project to the hypothalamus in the zebrafish (15). Thus, we sought to determine whether MC1R expression could be detected in zebrafish hypothalamus. For this experiment, tissues were dissected from three to nine adult zebrafish. Relative expression of the MC1R was higher in hypothalamus than skin or any other tissue tested (Fig. 6*A*), and expression in hypothalamus was higher than in brain tissue remaining after hypothalamic dissections. These data suggest that AgRP2-positive pineal neurons may project directly to MC1R-expressing neurons in the zebrafish hypothalamus (Fig. 6*B*).

Discussion

The two agouti proteins found in mammals, ASP and AgRP, acting as high-affinity endogenous antagonists of the melanocortin family of receptors (18, 20, 21), have been demonstrated to regulate the eumelanin–pheomelanin switch in mammalian pelage and long-term energy homeostasis, respectively. A gene encoding a third agouti protein, AgRP2, has been identified now in several fish species, including zebrafish, trout, Tetraodon, and Torafugu (22), and thus far seems unique to teleost fishes. This gene is likely to have arisen from the genome duplication that occurred during teleost phylogeny (35). In this study, we demonstrate a physiological function for this unique teleost-specific agouti protein: regulation of background adaptation.

Whole-mount in situ hybridization studies of 2- to 4-dpf embryos identified the pineal as the primary site of expression of the *agrp2* gene. qPCR identified the brain as the main site of expression of the gene in adult fish, although lower levels of expression were evident in skin, muscle, testis, and liver. *agrp2* mRNA was also identified in a transcriptomic analysis of the zebrafish pineal (36). Additionally, an immunohistochemical study also supports the hypothesis that AgRP2 protein is expressed in pineal but not in the retina, NLT, or other sites in the brain (37). An absence of retinal AgRP and AgRP2 immunoreactivity was observed in this study. Analysis of the promoter region of the zebrafish *agrp2* gene identified elements involved in pineal-specific expression, including PIPE, E-box, and PCE elements (38, 39). Thus, expression data, as well as data from the *flh* mutant described below, argue that the biological activities mediated by *agrp2* are mediated by expression of the protein by the pineal.

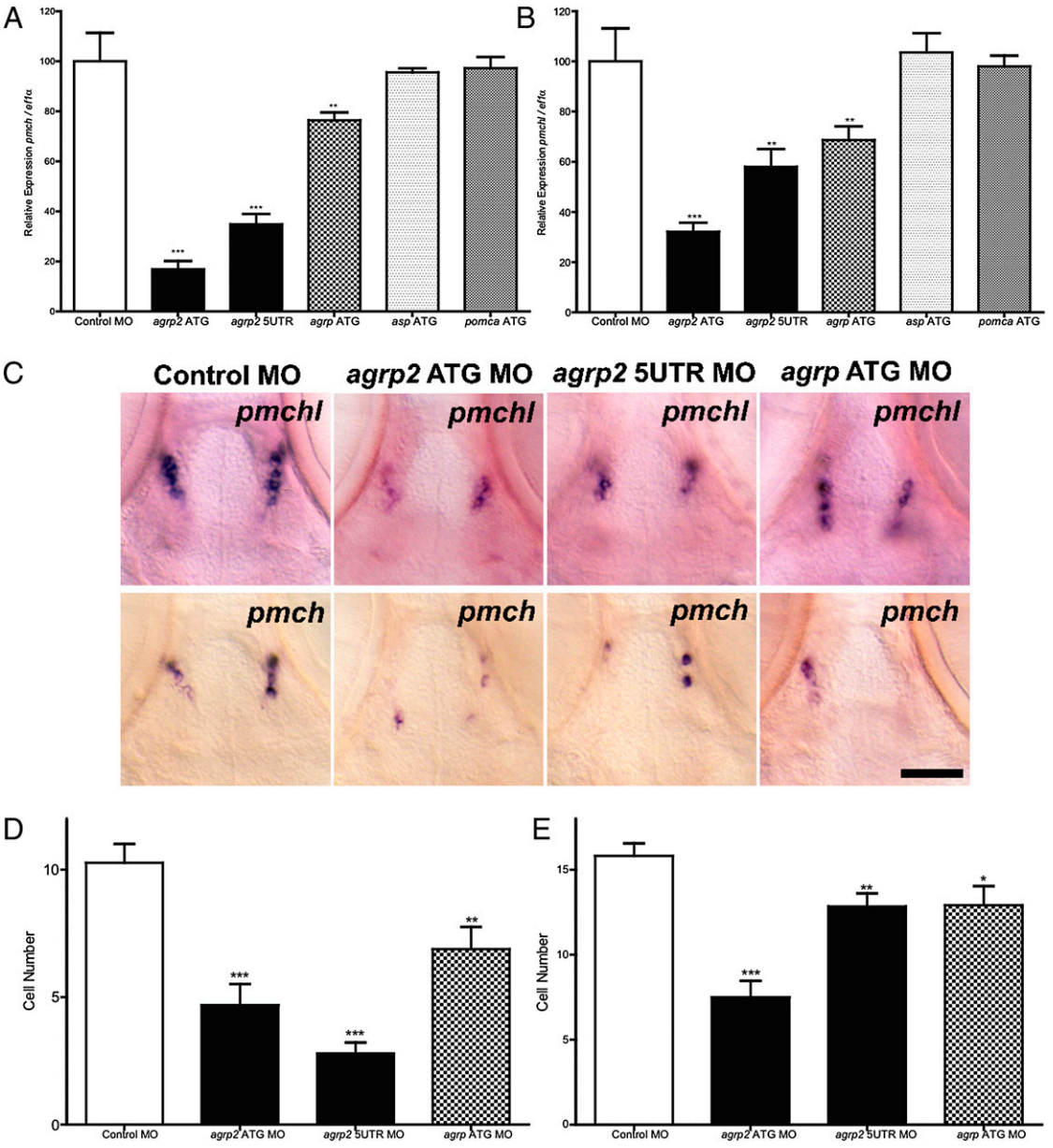

Fig. 4. *agrp2* regulates the expression of *pmch* and *pmchl* genes in the zebrafish. (*A* and *B*) Relative expression levels of *pmch* and *pmchl* were analyzed by qPCR. Two hundred wild-type zebrafish zygotes were injected with inverted *agrp2* ATG control MO, *agrp2* ATG MO, *agrp2* 5′ UTR MO, *agrp* ATG MO, *asp* ATG MO, and *pomca* ATG MO at day 0. Embryos were kept in egg water, changed daily, with 14-h/10-h light/dark cycle at 28 °C. Thirty embryos from each condition were divided into three groups and killed at 4 dpf (96 h) for RNA extraction and cDNA synthesis. Results are expressed as mean ± SEM, and statistical analysis was done by one-way ANOVA followed by Tukey posttest. $^{**}P < 0.01$; $^{***}P < 0.001$. (*C*) Whole-mount in situ hybridization for *pmch* (*Bottom*) or *pmchl* (*Top*) at 4 dpf after injection with inverted *agrp2* ATG control MO, *agrp2* ATG MO, *agrp2* 5′ UTR MO, or *agrp* ATG MO. After BM Purple AP staining, embryos were mounted in 2% methyl cellulose, and pictures were taken using AxionVision 3.1 software with a Lumar V12 stereo microscope (Carl Zeiss). At least 20 embryos for each condition were analyzed. (Scale bar: 50 μm.) (*D* and *E*) Numbers of *pmch*- and *pmchl*-expressing neurons at 4 dpf from fish injected with morpholinos described in *C* were counted with a stereomicroscope. Results are expressed as mean ± SEM, and statistical analysis was done by one-way ANOVA followed by Tukey posttest. $^{*}P < 0.05$; $^{**}P < 0.01$; $^{***}P < 0.001$. Numbers of fish analyzed and represented in each bar from left to right in *D* and *E* are 16, 14, 16, 15, 22, 19, 22, and 22, respectively.

In contrast to *agrp*, *agrp2* mRNA was not up-regulated by fasting. *agrp2* did not seem to be transcriptionally regulated by exposure of fish to white vs. black background and was only modestly regulated by diurnal rhythm (Fig. S3); in fact, diurnal effects on mRNA levels were only significant when fish were grown on a white background. Consequently, we hypothesize that the AgRP2 protein may be made constitutively, and a response to light may therefore involve the regulated release of AgRP2 from pineal neurons.

AgRP2 protein also exhibited a unique pharmacological profile, as determined by characterizing the ability of the folded zebrafish protein to inhibit the dose–response curve of α-MSH at the cloned zebrafish melanocortin receptors. Both zebrafish AgRP and AgRP2 acted as competitive antagonists and inverse agonists, shifting dose–response curves and suppressing the unique basal activity of the MC4R. However, whereas AgRP was a potent antagonist of the MC1R, MC3R, and MC4R, AgRP2 only exhibited potent antagonism of the MC1R, no antagonism of the MC3R, and two orders of magnitude lower potency than AgRP in antagonism of the MC4R.

These data implied a role for *agrp2* in the photosensitive control of pigmentation, because this is thought to be the exclusive physiological role of the MC1R. Adult zebrafish exhibit mela-

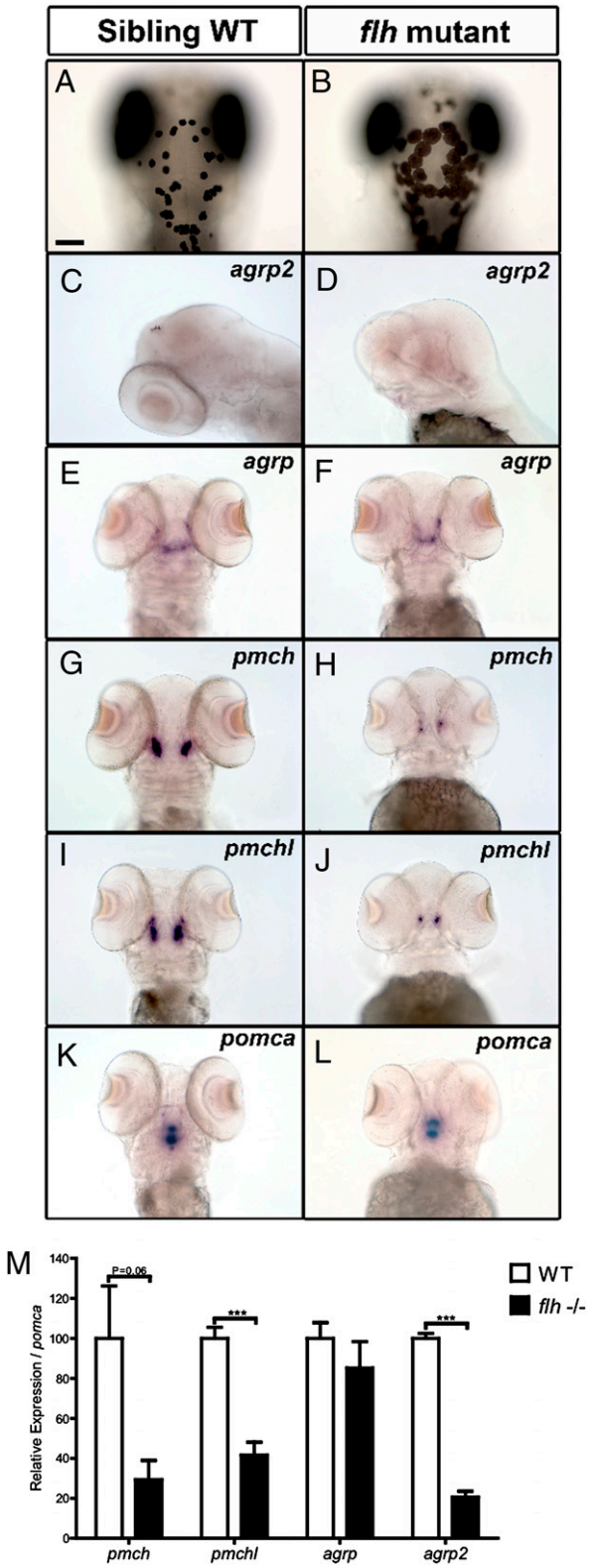

Fig. 5. *pmch, pmchl*, and *agrp2* are decreased in *floating head (flh)* mutants. $flh^{+/-}$ fish were crossed, and 400 zygotes were collected at 0 dpf, with 25% expected to be $flh^{-/-}$. Embryos were kept in egg water, changed daily, with 14-h/10-h light/dark cycle at 28 °C. Phenotypically wild-type or $flh^{-/-}$ embryos were fixed for whole-mount in situ hybridization (4 dpf) or killed for qPCR analysis (3 dpf). (*A* and *B*) Dorsal melanocytes of (*A*) white background-adapted sibling wild-type or (*B*) $flh^{-/-}$ embryos at 4 dpf. (*C–L*) Whole-mount in situ hybridization of (*C* and *D*) *agrp2*, (*E* and *F*) *agrp*, (*G* and *H*) *pmch*, (*I* and *J*) *pmchl*, and (*K* and *L*) *pomca* in white background-adapted sibling wild-type (*C*, *E*, *G*, *I*, and *K*) or $flh^{-/-}$ embryos (*D*, *F*, *H*, *J*, and *L*) at 4 dpf. At least 15 embryos for each condition were analyzed. (*M*) Relative expression levels of *agrp, agrp2, pmch*, and *pmchl* were analyzed by qPCR. Thirty $flh^{-/-}$ and 30 phenotypically wild-type embryos ($flh^{+/-}$ or $flh^{+/+}$) were divided into three groups and killed at 3 dpf for RNA extraction and cDNA synthesis. mRNA expression was normalized to *pomca* mRNA, and each expression level was further normalized to wild-type expression levels. Results are expressed as mean ± SEM, and statistical analysis was done by unpaired *t* test. ***$P < 0.001$. Scale bar: 100 μM.

nosome aggregation and up-regulation of MCH within 24 h of exposure to a white background. Zebrafish have two genes encoding MCH: *pmch* (most homologous to mammalian MCH, also called *pmch2*) and *pmchl* (also called *pmch1*), which seem to be expressed in different cells of the NLT (13). Berman et al. (13) found that expression of both *mch* genes was up-regulated under these conditions. We found that both melanosome aggregation and up-regulation of *pmch* and *pmchl* could also be demonstrated in zebrafish embryos after culture of the fish on a white background from fertilization to 4 dpf. Similar to the study in adults, we also found that *pmchl* was more significantly up-regulated than *pmch* (13). We also validated that background adaptation in embryos requires MCH, because morpholino knockdown of both *pmch* and *pmchl* reduced melanosome aggregation in embryos exposed to a white background (Fig. S5). Berman et al. (13) have suggested that *pmch* may play a more significant role in feeding behavior than *pmchl*, because peptide levels of the former were up-regulated by fasting in the zebrafish.

Although both MCH peptides may play a role in pigmentation, the role of agouti proteins in background adaptation seemed quite specific. Knockdown of *agrp2*, but not *agrp* or *asp*, blocked melanosome aggregation in response to a white background across the entire dermis of the fish (Fig. 3). Knockdown of *agrp2* also potently reduced *pmch* and *pmchl* expression, as measured by two different assays, qPCR and whole-mount in situ hybridization. Whereas knockdown of *asp* or *pomca* had no effect, it was interesting to note that knockdown of *agrp* expression did have a small effect on *pmch* and *pmchl* mRNA in the PCR assay. Because these MCH peptides may also play a role in food intake in the fish, this may be physiologically relevant; however, additional experiments would be required to rule out artifactual effects by which the *agrp* morpholinos may be acting. *pomca* also did not seem to be regulated by background. Thus, the production of MCH, but not *pomca*-derived α-MSH, seems to be transcriptionally regulated by exposure to light or dark background in a pineal and *agrp2*-dependent manner. Rather, data suggest that α-MSH release is up-regulated by exposure to a black background (10, 11), perhaps involving primarily nonvisual retinal phototransduction (Fig. 6*B*). Although these data demonstrate a neural mechanism of action for AgRP2 in the regulation of background adaptation, they do not test an additional complementary mechanism, secretion of AgRP2 by pineal neurons into the peripheral circulation allowing direct inhibition of melanosome dispersion via antagonism of MC1R on melanocytes.

floating head encodes a homeodomain protein, and absence of this gene product causes premature termination of pineal cell division at the 18 somite stage, ≈16–19 hpf. Data accumulated from the *floating head* mutant *flh* support the argument that the zebrafish pineal and pineal *agrp2* are necessary to allow melanosome aggregation and upregulation of *pmch* and *pmchl* when animals are grown on a white background. Again, *agrp* and *pomca* levels seem normal in *flh*, suggesting that *agrp2* and the pineal gland are not generally required for development of the NLT. *flh* does not seem to be expressed in the retina, and the CNS and retina seem to develop normally in *flh* animals (26), although it is not possible to rule out effects of *flh* on small numbers of photoreceptors in the retina.

Many blind zebrafish mutants have been demonstrated to exhibit defective background adaptation (29). However some of

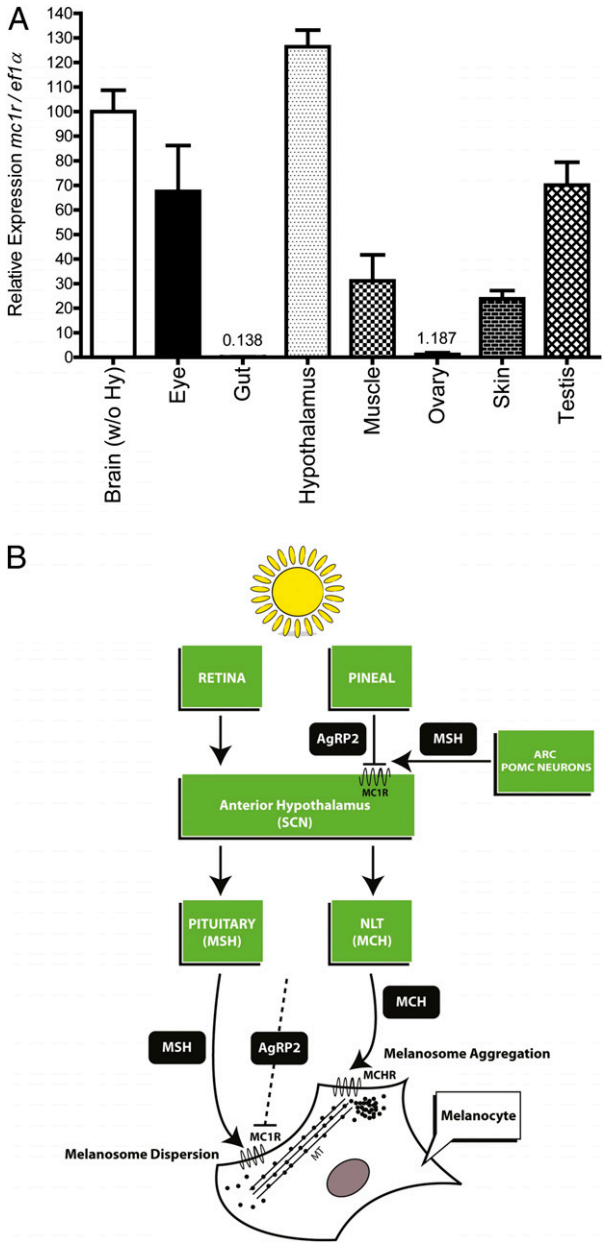

Fig. 6. *mc1r* is expressed in zebrafish hypothalamus. (*A*) Peripheral tissues and organs indicated were dissected from three 4-mo-old wild-type adults. Hypothalamus and brain tissue lacking hypothalamus were collected from nine 4-mo-old animals. Total RNA (600 ng) was extracted from each sample and used for cDNA synthesis. Expression level of *mc1r* mRNA, normalized to *ef1α*, was examined by qPCR. (*B*) Schematic view of neuroendocrine axes controlling backgound adaptation. Retina and pineal send information derived from photic signals to hypothalamic nuclei such as SCN. SCN and/or other hypothalamic nuclei then participate in relaying this information to pituitary and NLT to control the synthesis and/or release of α-MSH and MCH, respectively. Blockade of MC1R signaling by AgRP2 protein, after exposure to a white background, up-regulates *pmch* and *pmchl* mRNA levels in the NLT. Secretion of AgRP2 into the peripheral circulation (dashed lines, not yet tested) could also block the ability of MSH to stimulate melanosome dispersion by directly antagonizing the MC1R on melanocytes. Release of MCH and MCHL peptides results in melanosome aggregation; release of pituitary MSH results in melanosome dispersion. MCHR, MCH receptor; MT, microtubule.

these, such as *niezerka*, have mutations that result in the degeneration of both retinal and pineal photoreceptors (30). In contrast, the blind *nrc* mutant exhibits apparently normal pineal photoreceptors, as examined by electron microscopy (30). *nrc* encodes synaptojanin1, a polyphosphoinositide phosphatase involved in clathrin-mediated endocytosis that is required for proper structure and function of cone photoreceptor synapses (40). Thus, our data collected from these animals clearly show that visual phototransduction using cone photoreceptors is not required for melanosome aggregation, expression of *agrp2*, or up-regulation of *pmch* and *pmchl* expression by exposure to a white background. However, given the large percentage of blind mutants with defective background adaptation (29), it is evident that some aspect of retinal phototransduction, along with the pineal pathway described here, are required for regulation of *pmch* and *pmchl*. Indeed, retinal enucleation at 2 dpf also blocked the up-regulation of both *pmch* and *pmchl* by growth on a white background, as tested by qPCR at 5dpf (Fig. S7).

The data here thus identify a unique physiological function for a third member of the family of agouti proteins, AgRP2, which seems to be specific to teleosts. These data also identify a unique neuroendocrine circuit defined by *agrp2*-positive pineal neurons that regulate *pmch* and *pmchl* expression in neurons in the lateral tuberal nucleus of the fish in response to environmental background. Transcriptional upregulation and increased release of MCH peptides from these hypophysiotrophic neurons in the NLT in turn is required for melanosome contraction. The data do not allow us to determine whether the pineal *agrp2* neurons project directly to the MCH expressing neurons of the NLT, or to an intermediate site, such as the SCN. The existing anatomical data, showing pineal fibers in the anterior hypothalamus but not the NLT, argue for a multisynaptic circuit (15). Given the pharmacological characterization of AgRP2 as an MC1R antagonist, it may be possible to identify the relevant intermediate neurons by identifying cells that express the MC1R and also receive pineal projections expressing AgRP2. Although the data here show a clear role for the pineal in background adaptation, via regulation of MCH expression, and no role for visual phototransduction by cone photoreceptors, nonvisual retinal phototransduction is also implicated in the process (29). The process of background adaptation, with neuroanatomically distinct pathways regulating α-MSH release from the pituitary and MCH release from the hypothalamus, is complex, and the specific contributions of and interactions between retinal nonvisual phototransduction and pineal phototransduction in this process remain to be determined.

Materials and Methods

Experimental Animals. Wild-type Tab 14 or AB strain zebrafish, *flh* mutants [allele: *n1*; Zebrafish Model Organism Database (ZFIN) ID: ZDB-ALT-980203-470], and nrc mutants [allele: *tQ296x(JV039)*; ZFIN ID: ZDB-ALT-100510-1] were raised and bred as described (*SI Materials and Methods*).

Isolation of Total RNA and cDNA Synthesis. Total RNA was extracted using TRIzol LS reagent (Invitrogen) according to the manufacturer's instruction. To remove genomic DNA, purified total RNA was treated with RNase free DNase (Roche) at 37 °C for 30 min and cleaned with RNeasy mini kit (Qiagen) according to the manufacturer's instructions. Purified total RNA (1 μg) was reverse-transcribed with oligo dT primers using a first-strand cDNA synthesis kit (Fermentas).

Whole-Mount in Situ Hybridization. Full-length *agrp2, pmch, pmchl,* and *pomca* sequences were cloned into pCR4-TOPO vector (Invitrogen) using primers in which the first six nucleotides of each primer encode a BamHI or NOT1 restriction site (*SI Materials and Methods*). Digoxygenin cRNA probes were synthesized, and whole mount in situ hybridizations were performed as described in *SI Materials and Methods*.

Fasting and Feeding Experiments. For fasting experiments, to minimize contamination with microorganisms, fish system water was filter-sterilized with a 0.2-μm supor membrane (Pall). For fasting experiments, approximately 10 adult male fish, aged 10–12 mo, were grouped in one tank filled with filter-sterilized fish system water and manually supplied with fresh filtered system water every other day. At days 5, 10, and 15 of fasting, fish were anesthetized with ice, and whole intact brain tissue was dissected. Dissected brain tissues

were immediately put in 0.6 mL of TRIzol reagent, homogenized with a 20-G syringe, and kept at −80 °C until used for preparation of RNA.

Real-Time qPCR. qPCR primers were designed by Beacon Designer 7.0 (Premier Biosoft International) to minimize primer self-dimerization (see *SI Materials and Methods* for primer sequences). qPCRs were performed as described in *SI Materials and Methods*.

Construction and Use of Melanocortin Receptor Expression Vectors. Zebrafish melanocortin receptor 1 was amplified from skin cDNA according to the published sequences. PCR products were subcloned into the pcDNA3.1+ vector using BamH I and EcoR I sites. Zebrafish melanocortin receptor 3 was kindly provided by Dr. Darren Logan (Western General Hospital, Edinburgh, United Kingdom). pGEMT-zMC3R was digested by Not I enzyme and subcloned into pcDNA3.1+ using the same restriction site. Zebrafish melanocortin receptor 4, 5a, and 5b were independently cloned from a zebrafish brain cDNA library. Zebrafish melanocortin receptor 4 and 5a were subcloned into pcDNA3.1+ using a BamH I site, and zebrafish melanocortin receptor 5b was cloned into pcDNA3.1+ using a Not I site. Stable transfectants were made in HEK-293 cells using lipofectamine or lipofectamine2000 (Invitrogen), followed by selection in 1,000 μg/mL G418.

Peptide Synthesis, Purification, and Folding. Zebrafish AgRP (Ac-83-127-NH_3) and AgRP2 (Ac-Y-94-136-NH_3) were synthesized using Fmoc synthesis on an Applied Biosystems 433A Peptide Synthesizer on a 0.25-mmol scale and folded into biologically active forms (see *SI Materials and Methods* for details). Reinjecting a small sample of the purified peptide on an analytical RP-HPLC column assessed purity of the peptides. The purity of both peptides was determined to be >85%. Quantitative analysis of the peptide concentrations was done by amino acid analysis at the molecular structure facility at University of California, Davis.

β-Galactosidase Assay. Zebrafish melanocortin receptor activity was measured using a cAMP-dependent β-galactosidase assay in HEK-293 cell transfectants as described previously (42). Cells were incubated with serially diluted concentrations of α-MSH in the presence or absence of $zAgRP_{(83–127)}$ or $zAgRP2_{(93-136)}$ in a final 50-μL volume using a 96-well format. Color development was measured at 405 nm with a Benchmark Plus plate spectrophotometer (Bio-Rad).

Design and Injection of MO. Antisense MOs were designed and synthesized from GeneTools (*SI Materials and Methods*). MOs were dissolved in nuclease-free water (Promega) and stored in −20 °C as 1 mM stock for later use, as described (*SI Materials and Methods*).

ACKNOWLEDGMENTS. We thank Teresa Nicholson (Vollum Institute, Oregon Health & Science University, Portland, OR) for providing the *nrc* mutant embryos; and Rob Duncan and Savannah Williams for technical assistance. This work was supported by National Institutes of Health (NIH) Grant DK075721 (to R.D.C.), a Freedom to Discover Grant from the Bristol-Myers Squibb Foundation (to R.D.C.), and by NIH Grants DK64265 (to G.M.), DC04186 (to M.W.), and HD22486 (to M.W.).

1. Berson DM, Dunn FA, Takao M (2002) Phototransduction by retinal ganglion cells that set the circadian clock. *Science* 295:1070–1073.
2. Freedman MS, et al. (1999) Regulation of mammalian circadian behavior by non-rod, non-cone, ocular photoreceptors. *Science* 284:502–504.
3. Lucas RJ, Freedman MS, Muñoz M, Garcia-Fernández JM, Foster RG (1999) Regulation of the mammalian pineal by non-rod, non-cone, ocular photoreceptors. *Science* 284: 505–507.
4. Gooley JJ, Lu J, Fischer D, Saper CB (2003) A broad role for melanopsin in nonvisual photoreception. *J Neurosci* 23:7093–7106.
5. Peirson SN, Halford S, Foster RG (2009) The evolution of irradiance detection: Melanopsin and the non-visual opsins. *Philos Trans R Soc Lond B Biol Sci* 364: 2849–2865.
6. Provencio I, Jiang G, De Grip WJ, Hayes WP, Rollag MD (1998) Melanopsin: An opsin in melanophores, brain, and eye. *Proc Natl Acad Sci USA* 95:340–345.
7. Breder CM, Rasquin P (1950) A preliminary report on the role of the pineal organ in the control of pigment cells and light reactions in recent teleost fishes. *Science* 111:10–12, illust.
8. Kawauchi H, Kawazoe I, Tsubokawa M, Kishida M, Baker BI (1983) Characterization of melanin-concentrating hormone in chum salmon pituitaries. *Nature* 305:321–323.
9. Lee TH, Lerner AB (1956) Isolation of melanocyte-stimulating hormone from hog pituitary gland. *J Biol Chem* 221:943–959.
10. Baker BI (1981) Biological role of the pars intermedia in lower vertebrates. *Ciba Found Symp* 81:166–179.
11. Baker BI, Wilson JF, Bowley TJ (1984) Changes in pituitary and plasma levels of MSH in teleosts during physiological colour change. *Gen Comp Endocrinol* 55:142–149.
12. Amano M, Takahashi A (2009) Melanin-concentrating hormone: A neuropeptide hormone affecting the relationship between photic environment and fish with special reference to background color and food intake regulation. *Peptides* 30: 1979–1984.
13. Berman JR, Skariah G, Maro GS, Mignot E, Mourrain P (2009) Characterization of two melanin-concentrating hormone genes in zebrafish reveals evolutionary and physiological links with the mammalian MCH system. *J Comp Neurol* 517:695–710.
14. Mano H, Fukada Y (2007) A median third eye: Pineal gland retraces evolution of vertebrate photoreceptive organs. *Photochem Photobiol* 83:11–18.
15. Yáñez J, Busch J, Anadón R, Meissl H (2009) Pineal projections in the zebrafish (*Danio rerio*): Overlap with retinal and cerebellar projections. *Neuroscience* 164:1712–1720.
16. Bultman SJ, Michaud EJ, Woychik RP (1992) Molecular characterization of the mouse agouti locus. *Cell* 71:1195–1204.
17. Miller MW, et al. (1993) Cloning of the mouse agouti gene predicts a secreted protein ubiquitously expressed in mice carrying the lethal yellow mutation. *Genes Dev* 7: 454–467.
18. Ollmann MM, et al. (1997) Antagonism of central melanocortin receptors in vitro and in vivo by agouti-related protein. *Science* 278:135–138.
19. Shutter JR, et al. (1997) Hypothalamic expression of ART, a novel gene related to agouti, is up-regulated in *obese* and *diabetic* mutant mice. *Genes Dev* 11:593–602.
20. Lu D, et al. (1994) Agouti protein is an antagonist of the melanocyte-stimulating-hormone receptor. *Nature* 371:799–802.
21. Fong TM, et al. (1997) ART (protein product of agouti-related transcript) as an antagonist of MC-3 and MC-4 receptors. *Biochem Biophys Res Commun* 237:629–631.
22. Kurokawa T, Murashita K, Uji S (2006) Characterization and tissue distribution of multiple agouti-family genes in pufferfish, *Takifugu rubripes*. *Peptides* 27:3165–3175.
23. Song Y, Golling G, Thacker TL, Cone RD (2003) Agouti-related protein (AGRP) is conserved and regulated by metabolic state in the zebrafish, *Danio rerio*. *Endocrine* 22:257–265.
24. Song Y, Cone RD (2007) Creation of a genetic model of obesity in a teleost. *FASEB J* 21:2042–2049.
25. Bolin KA, et al. (1999) NMR structure of a minimized human agouti related protein prepared by total chemical synthesis. *FEBS Lett* 451:125–131.
26. Masai I, et al. (1997) floating head and masterblind regulate neuronal patterning in the roof of the forebrain. *Neuron* 18:43–57.
27. Halpern ME, et al. (1995) Cell-autonomous shift from axial to paraxial mesodermal development in zebrafish floating head mutants. *Development* 121:4257–4264.
28. Li L, Dowling JE (1997) A dominant form of inherited retinal degeneration caused by a non-photoreceptor cell-specific mutation. *Proc Natl Acad Sci USA* 94:11645–11650.
29. Neuhauss SC, et al. (1999) Genetic disorders of vision revealed by a behavioral screen of 400 essential loci in zebrafish. *J Neurosci* 19:8603–8615.
30. Allwardt BA, Dowling JE (2001) The pineal gland in wild-type and two zebrafish mutants with retinal defects. *J Neurocytol* 30:493–501.
31. Mountjoy KG, Robbins LS, Mortrud MT, Cone RD (1992) The cloning of a family of genes that encode the melanocortin receptors. *Science* 257:1248–1251.
32. Robbins LS, et al. (1993) Pigmentation phenotypes of variant extension locus alleles result from point mutations that alter MSH receptor function. *Cell* 72:827–834.
33. Klovins J, et al. (2004) The melanocortin system in Fugu: Determination of POMC/AGRP/MCR gene repertoire and synteny, as well as pharmacology and anatomical distribution of the MCRs. *Mol Biol Evol* 21:563–579.
34. Selz Y, et al. (2007) Evolution of melanocortin receptors in teleost fish: The melanocortin type 1 receptor. *Gene* 401:114–122.
35. Taylor JS, Braasch I, Frickey T, Meyer A, Van de Peer Y (2003) Genome duplication, a trait shared by 22000 species of ray-finned fish. *Genome Res* 13:382–390.
36. Toyama R, et al. (2009) Transcriptome analysis of the zebrafish pineal gland. *Dev Dyn* 238:1813–1826.
37. Forlano PM, Cone RD (2007) Conserved neurochemical pathways involved in hypothalamic control of energy homeostasis. *J Comp Neurol* 505:235–248.
38. Asaoka Y, Mano H, Kojima D, Fukada Y (2002) Pineal expression-promoting element (PIPE), a cis-acting element, directs pineal-specific gene expression in zebrafish. *Proc Natl Acad Sci USA* 99:15456–15461.
39. Appelbaum L, Gothilf Y (2006) Mechanism of pineal-specific gene expression: The role of E-box and photoreceptor conserved elements. *Mol Cell Endocrinol* 252:27–33.
40. Van Epps HA, et al. (2004) The zebrafish nrc mutant reveals a role for the polyphosphoinositide phosphatase synaptojanin 1 in cone photoreceptor ribbon anchoring. *J Neurosci* 24:8641–8650.
41. Kimmel CB, Ballard WW, Kimmel SR, Ullmann B, Schilling TF (1995) Stages of embryonic development of the zebrafish. *Dev Dyn* 203:253–310.
42. Chen W, Shields TS, Stork PJ, Cone RD (1995) A colorimetric assay for measuring activation of Gs- and Gq-coupled signaling pathways. *Anal Biochem* 226:349–354.